

## MULTICAVITY PROTON CYCLOTRON ACCELERATOR\*

Changbiao Wang<sup>1</sup>, V. P. Yakovlev<sup>2</sup>, and J. L. Hirshfield<sup>1,2</sup>

<sup>1</sup>Department of Physics, Yale University, New Haven, CT 06520-8120, USA

<sup>2</sup>Omega-P, Inc., 199 Whitney Ave., New Haven, CT 06511, USA

### Abstract

Analysis is presented for a multicavity proton cyclotron accelerator in which a 122 mA, 1 MeV proton beam is accelerated to 954 MeV using a cascade of eight cavities in an 8.1 T magnetic field, with effects of finite beam radius and velocity and energy spreads taken into account. The first cavity operates at 120 MHz, and successive cavities have resonance frequencies lower in increments of 8 MHz. For this example, average acceleration gradient exceeds 37.9 MV/m, average effective shunt impedance is 207 MΩ/m, but maximum surface field in the cavities does not exceed 7.2 MV/m. Such an accelerator might be suitable for driving a high-power neutron spallation source.

### INTRODUCTION

Intense proton beams are needed in a wide variety of applications in high-energy physics, including production of elementary particles such as kaons, pions, muons, and neutrinos [1]. A 10-30 GeV proton accelerator with mA-level current will be required for a future muon collider [2]. 0.5-2.5 GeV high intensity proton beams could also be required with beam powers exceeding 100 MW for neutron production by spallation for several critical applications, such as accelerator production of tritium [3] and accelerator-driven transmutation of nuclear waste [4]; current machines operate at about 1 MW [5].

The multi-cavity proton cyclotron (MCPC) has been proposed and analyzed for high-efficiency, high-gradient acceleration of a high-current proton beam in a normal conducting structure [6-8]. It has been shown that a proton beam can be accelerated in the MCPC from 1 MeV to ~1 GeV with more than 100 MW beam power [8]. The new concept is based on use of a cascade of rotating-mode normal conducting TE<sub>111</sub> cavities in a strong nearly-uniform static magnetic field. Cyclotron-resonance acceleration in each cavity provides energy gain for the protons. The cavity resonance frequencies  $f_n$  decrease from  $f_1$  for the first cavity, with a fixed frequency interval  $\Delta f$  between each of the  $N$  cavities; thus  $f_n = f_1 - (n-1)\Delta f$  and  $f_1 = l\Delta f$ , with the integer  $l \geq n$ , and  $1 \leq n \leq N$ . Proton pulses are injected into the first cavity at intervals  $\Delta T = 1/\Delta f$  or integer multiples thereof.

Based on the previous study [8], an example is presented below with the effects of beam spreads in velocity, energy, and radius taken into account. The effect of drift tunnels between cavities is also included and the phase angle of injection of proton beam is optimized. Simulations show that a 122-mA, 1-MeV proton beam is accelerated to 954 MeV using a cascade of

eight regular TE<sub>111</sub> cavities in an 8.1 T magnetic field and the performance of the MCPC is not so significantly affected by these effects for a beam with reasonable spread parameters. It is also found that this acceleration mechanism can be sustained for an exceptionally wide injection phase angle in the first cavity, e.g., two rf cycles (16.7 ns), compared to 0.3 of an rf cycle (2.5 ns) in the previous work [8]. This feature is highly significant, in that it allows operation with high duty factor (~13%) and low peak proton current (<1 A), thereby mitigating against issues that can arise from high beam space charge.

In addition, the effect on proton dynamics of the apertures and drift tunnels for a beam traversing cavities is also examined by use of realistic rf fields in place of analytic field forms for idealized cavities.

### SIMULATION ANALYSIS

The cascade of eight TE<sub>111</sub> cavities in the MCPC example has a frequency separation of  $\Delta f = 8$  MHz and resonant frequencies of 120, 112..., and 64 MHz. Thus 15, 14..., and 8 full rf cycles pass in these cavities, respectively, between proton bunches when they are injected every 125 ns (i.e., at an 8 MHz rate). Average beam current is chosen to be 122 mA, injected in 16.7 nsec bunches (two rf cycles in the first cavity), and thus with a peak current of 0.915 A (duty factor = 1/7.5); the energy of the injected proton beam is taken to be 1 MeV.

In simulations, 20-cm drift tunnels between cavities are added to isolate cavity fields from one another; an injected proton beam with finite spreads in energy, velocity and radius is introduced. The parameters for the spreads are chosen by reference to those for an ideal solid Brillouin beam of radius  $r_b$  [m] with the specified peak current  $I$  [A] in the specified magnetic field  $B_z$  [T]. Here the magnetic field  $B_z$  (7.9 T) can be obtained from the gyro-resonant condition for the first cavity, and the beam radius is chosen to be 0.9 mm from Brillouin beam condition, given by  $r_b B_z = (240 I U_p / \gamma \beta c^2)^{1/2}$ , where  $U_p$  is the particle rest energy expressed in eV ( $938.2 \times 10^6$  eV for proton),  $\gamma$  and  $\beta$  are the relativistic energy factor and normalized velocity on the axis for the beam, and  $c$  is the speed of light in m/s. For the solid Brillouin beam, the across-beam voltage depression caused by space charge is given by  $30I/\beta$ , and it is 0.6 kV for a beam with energy 1 MeV and peak current 0.915 A. The beam energy spread is chosen to be 1.2 keV (=0.37 keV in rms spread), double the above beam energy depression. The normalized transverse velocity spread can be estimated from  $\Delta\beta_{\perp} \approx (2\Delta\gamma / \langle\gamma\rangle)^{1/2} / \langle\gamma\rangle \approx (2\Delta\gamma)^{1/2}$  with  $\langle\gamma\rangle$  the average energy factor; it is chosen to be  $1.3 \times 10^{-3}$ , corresponding to rms spread  $6.5 \times 10^{-4}$ . According to

\*Work supported by US DoE.

$30I/\beta[1+2\ln(R_w/r_b)]$  where  $R_w$  is the first cavity radius (92 cm), the full voltage depression is 8.8 kV, much less than the beam voltage 1 MV, and the space charge effect on particle dynamics is negligible. Beam parameters in simulations are listed in Table 1.

Table 1: Proton Beam Parameters in Simulations

initial beam energy	1 MeV
initial beam velocity	$0.0461c$
peak beam current $I$	0.915 A
average beam current $\langle I \rangle$	0.122 A
pulse period	125 nsec
pulse duration	16.7 nsec
duty factor	$1/7.5 = 13.3\%$
beam radius $r_b$	0.9 mm
beam energy spread	1.2 keV
rms perpendicular velocity spread	$6.5 \times 10^{-4} c$

Analytic field expressions for TE<sub>111</sub> mode [8] are used and the intrinsic (ohmic) quality factors  $Q_0$  for the cavities are calculated assuming copper construction. Simulations show that the peak surface electric fields range from 3.9 to 7.2 MV/m, well below breakdown. Specific cavity parameters and mean acceleration energy gains for each of the eight stages are given in Table 2.

Fig. 1 shows the dependence of average energy factor and axial magnetic field on axial distance. The magnetic field traversing the cavities varies mildly in the range 7.9-8.2 T for optimum energy gain, and the average energy factor is increased from 1.0011 (1 MeV) to 2.0164 (953.7 MeV). The final beam power is 116.2 MW, rf-to-beam power efficiency is 66.8%, and average effective acceleration gradient is 37.9 MV/m, as compared with 40.4 MeV/m for a zero-spread beam without drift tunnels [8]. Most of this decrease is due to the 140-cm increase in machine length from adding the drift tunnels.

Fig. 2 shows the dependence of rms  $\gamma$  and  $\beta_z$ -spreads on axial distance  $z$ . The energy factor spread is increased from initial  $3.9 \times 10^{-7}$  (0.37 keV) to 0.0063 (6 MeV) at the end of the device, and the axial velocity spread is increased from  $9.2 \times 10^{-6}c$  to  $0.0040c$ , compared with 0.0026 (2.4 MeV) and  $0.0012c$  at the end respectively for the zero-spread beam example [8].

Table 2: Parameters for a 122 mA, 8-Cavity Proton Cyclotron

stage #	cavity frequency (MHz)	cavity radius (cm)	cavity length (m)	rf power input (MW)	relative rf phase	beam-loaded cavity $Q_L$	intrinsic cavity $Q_0$ (copper)	peak surface field (MV/m)	mean energy gain (MeV)
1	120	92	2.06	18.0	0	$6.25 \times 10^4$	$1.1 \times 10^5$	7.2	63.6
2	112	98	2.23	15.0	$1.40\pi$	$2.68 \times 10^4$	$1.1 \times 10^5$	4.0	92.9
3	104	106	2.39	15.5	$1.45\pi$	$4.36 \times 10^4$	$1.2 \times 10^5$	4.8	80.9
4	96	110	2.81	18.5	$1.85\pi$	$4.39 \times 10^4$	$1.2 \times 10^5$	4.9	96.1
5	88	120	3.07	24.0	$0.50\pi$	$4.41 \times 10^4$	$1.2 \times 10^5$	5.1	124.3
6	80	132	3.38	23.0	$1.70\pi$	$3.67 \times 10^4$	$1.3 \times 10^5$	4.1	135.3
7	72	144	3.92	30.0	$0.15\pi$	$3.65 \times 10^4$	$1.3 \times 10^5$	4.2	177.0
8	64	172	3.89	30.0	$0.55\pi$	$3.85 \times 10^4$	$1.5 \times 10^5$	3.9	182.7
total			25.15	174.0					952.7

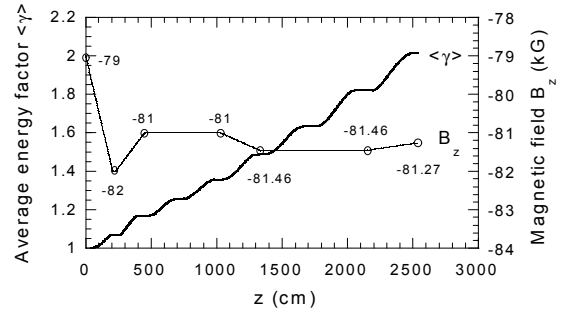


Figure 1: Dependence of average energy factor  $\langle \gamma \rangle$  and axial magnetic field  $B_z$  on axial distance  $z$ . In the 20-cm drift regions the magnetic field is uniform.

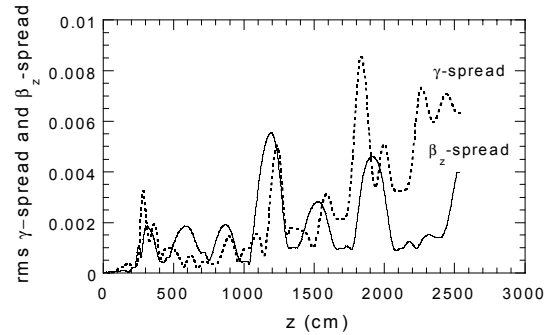


Figure 2: Dependence of rms energy factor and normalized axial velocity spreads on axial distance.

## INFLUENCE OF APERTURES AND TUNNELS ON PARTICLE DYNAMICS

Although the effect of protons drifting through tunnels between cavities is considered in the above analysis, the modification of rf fields by the apertures on cavity end walls and by the tunnels is not included. Proton dynamics will be influenced by this modification. To gauge this influence, a study that uses realistic fields was done for the first three stages with a 122-A, 1-MeV zero-spread proton beam, for comparison with a study that uses analytic field expressions for idealized cavities. Table 3 shows the simulation results for the two cases: *case a* corresponds to analytic field expressions used and *case b*

Table 3: Simulation Results for the First Three Cavities for *Case a* and *Case b*

	120 MHz cavity		112 MHz cavity		104 MHz cavity	
	<i>case a</i>	<i>case b</i>	<i>case a</i>	<i>case b</i>	<i>case a</i>	<i>case b</i>
energy gain (MeV)	63.6	64	92.9	93	80.9	80
maximum $E_{\perp}$ (MV/m)	11.3	11.3	6.3	8.14	7.6	9.4
unloaded quality factor	110,000	109,000	110,000	111,000	120,000	11,600
power applied (MW)	18	18	15	17	15.5	19
power dissipated (MW)	10.2	10	3.7	6	5.6	9.5

corresponds to realistic fields used [9].

In simulations, the energy gains are adjusted to be the same for the two cases. From Table 3, it is seen that almost nothing is affected for the first cavity. Compared to *case a*, the input rf power for *case b* is increased by 13.3% for the second cavity while 22.6% for the third, with more power lost to the walls.

Fig. 3 shows the dependence of energy  $E$  and radial coordinate  $R$  on axial distance  $z$  for individual particles for *case b*, with cavity and drift outlines shown to scale. It is seen that all the particles go through the cavities without hitting any walls.

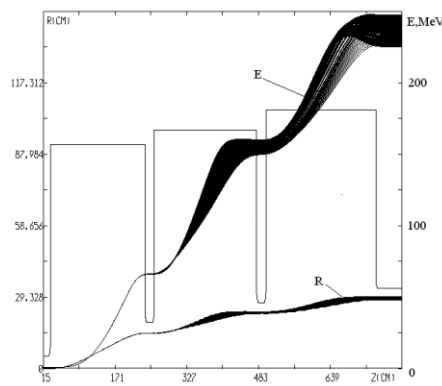


Figure 3: Energy and radius *versus*  $z$  for accelerated protons in a zero-velocity-and-radius-spread beam for *case b*. Peak current  $I = 915$  mA, and duty = 1/7.5. Cavity and drift tunnel outlines are shown to scale.

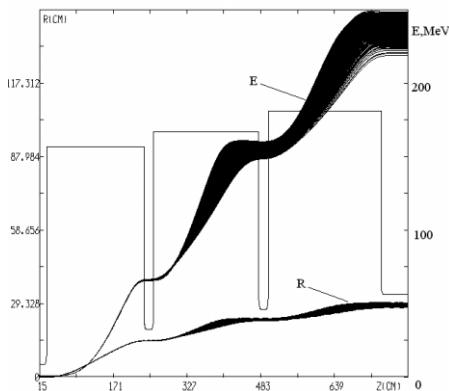


Figure 4: Energy and radius *versus*  $z$  for accelerated protons in a beam with velocity, energy, and radius spreads for *case c*. Peak current  $I = 915$  mA and duty = 1/7.5. Cavity and drift tunnel outlines are shown to scale.

*Case c* is an example where realistic rf fields like *case b* are employed for a beam with parameters given by Table 1 except the energy spread is 0.6 keV. The results are shown in Fig. 4, for comparison with the above zero-spread beam *case b*. It is seen from Fig. 4 that the energy curves for individual particles spread wider than *case b*, leading to a bigger energy spread, but their average energy is almost the same, about 238 MeV.

## REMARK

The new proton accelerator concept MCPC presented here could form the basis for an alternative to a superconducting linac for production of high-intensity proton beams, either for a K-factory or a  $\Pi$ -factory, in a muon collider, or in a neutron spallation source such as that needed for driving a sub-critical reactor for accelerator-based transmutation of nuclear waste.

## REFERENCES

- [1] J. L. Laclare, "CONCERT a high power proton accelerator driven multi-application facility concept," IEEE NSS-MIC, Lyon, France, Oct. 15-20, 2000.
- [2] C. M. Ankenbrandt et al., Phys. Rev. ST Accl. Beams 2, (1999) 081001.
- [3] J. L. Anderson, P. W. Lisowski, W. P. Bishop, J. T. McCormack, and J. G. Angelos, "Status of the accelerator production of Tritium (APT) project," in Proc. of the 3rd Int. Conf. on ADTTA, Praha (Pruhonice), Czech, June 7-11, 1999.
- [4] G. P. Lawrence, "High-power proton linac for transmuted the long-lived fission products in nuclear waste," in Proc. of PAC'1991, p. 2598.
- [5] W. Chou, "Spallation neutron source and other high intensity proton sources," A lecture at the 3rd OCPA Int. Accel. School, Singapore, Jul. 25-Aug. 3, 2002.
- [6] J. L. Hirshfield, C. Wang, and R. Symons, in AAC: 9th Workshop, AIP Conf. Proc. 569 (AIP, New York, 2001), p. 833.
- [7] C. Wang and J. L. Hirshfield, in Proc. of PAC'2001, p. 3389.
- [8] J. L. Hirshfield, C. Wang, and V. P. Yakovlev, Phys. Rev. ST Accel. Beams 5, (2002) 081301.
- [9] V. P. Yakovlev, O. A. Nezhevenko, O. V. Danilov, D. G. Myakishev, and M. A. Tiunov, in AAC: 10th Workshop, AIP Conf. Proc. 647 (AIP, New York, 2002), p. 421.